

Supplementary Information for

Timing Facilitated Site Transfer of an Enzyme on DNA

Joseph D. Schonhoft and James T. Stivers

Supplementary Methods

Oligonucleotide Reagents

All DNA substrates listed below were purchased from Integrated DNA Technologies (www.IDTDNA.com) and purified by denaturing polyacrylamide gel electrophoresis. For all duplex substrates an adenine was placed opposite to uracil in the complementary strand.

125mer-55 bp U separation (S55)

GGT ATC CGC TCA CAA TTC CAC ACA ATG CTG AGG AAT CGA U AGC TAA GTG
AAT CTC TCA CGT CAC ATC GTC CGC ACT AGC ACA TGG AAT GAA TCG A U
AGC TAA GCT GAG GCA TAC AGT GTC GAG CC

90mer-20 bp U separation (S20)

5' - GGT ATC CGC TCA CAA TTC CAC ACA ATG CTG AGG AAT CGA U AG CTA
AGT AGG ATG AAT CGA U AG CTA AGC TGA GGC ATA CAG TGT CGA GCC

90mer-10 bp U separation (S10)

5' - GGT ATC CGCT AGT CAC AAT TCC ACA CAATGC TGA GGA ATC GA U AG
CTA AT CGA U AGC TAA GCT GAG GCATAC AGG ATC AAT TGT CGA GCC

90mer-6 bp U separation (S6)

5' - GGT ATC CGC TGA AGT AGT CAC AAT CCA CAC AAT GCT GAG GAA TCG
AUA GCC GAU AGC TAA GCT GAG GCA TAC AGG ATC AAT TGT CGA GCC

90mer-5 bp U separation (S5)

5' - GGT ATC CGC TGAA GTA GTC ACA ATT CCA CAC AAT GCT GAG GAA TCG
AUA GCG AUA GCT AAG CTG AGG CAT ACA GGA TCA ATT GTC GAG CC

90mer-5 bp U separation on opposite strands (S5^{opp})

5' - GGC TCG ACA AGC TCT CAT CTG TGC TGA GGA TGT TAG CTU AGG CTA
TCG ATT CCT CAG CAT TGT GTG GAG ACA CCT TTG TGA GCG GAT ACC
(underlined A indicates position of the uracil on the complementary strand)

90mer-5bp U single strand (S5^{ss})

5' - ACC ATA ATA ATA ACA CAT ACA CCA TAC TAC ATA CAT CAA CTA AAA CAU
ACA CAU ACA AAA TCA ACT AAT AAC AAC ACATAC ACC ATA ACA

90mer-10bp U single strand (S10^{SS})

CAC AAT AAC ACA TAC ACC ATA CTA CAT ACA TCA ACT AAA ACA UAC ACA
ACA CAU ACA AAA TCA ACT AAT AAC AAC ACA TAC ACC ATA ACA

Non-specific duplex (nsDNA)

3' - C GCG TGT GCC

5' - G CGC ACA CGG - FAM

90mer- 1 uracil site (1XU)

5' - GTT ATC CGC TCA CAA TTC CAC ACA ATG CTG AGG AAT CGA UAG CTA
AGT AGG ATG TTA GCT ATC GAT TCA TCC TCA GCA CAG TGT CGA GCC

Chase duplex (chDNA)

5' - GCG GCC AAA ϕ AA AAA GCG C

3' - GCG GCC AAA A TT TTT CGC G

(ϕ - tetrahydrofuran abasic site mimic)

Efficiency of Uracil Excision by hUNG

The efficiency of uracil excision by hUNG when it lands on a uracil site is determined by the ratio of the excision rate (k_{ex}) to the off-rate (k_{off})². This efficiency was determined by a pulse-chase kinetic partitioning experiment². Using a three syringe rapid mixing apparatus (Kintek RQF3), 2 μM of hUNG solution was rapidly mixed with 40 nM of a uracil-containing 90mer duplex substrate (1XU) labeled with ³²P at the 5' terminus. After 2 ms aging time the reaction was quenched with either 0.5 M HCl or 60 μM of a 19mer chase DNA duplex (chDNA) containing a tetrahydrofuran abasic site product analogue. Under these high chase DNA concentrations, the trapping of the enzyme is independent of the chDNA concentration. For the acid quenched samples an equal volume of phenol/chloroform/isoamylalcohol (25:24:1, Invitrogen) was added and followed by vortexing. The sample was then centrifuged to separate aqueous and organic phases and 50 μl of the aqueous layer was transferred to a clean tube. 5 μl of 10 M piperidine was then added and the solution was heated to 90 °C for 20 minutes to cleave abasic sites. For the reactions that were quenched with the chDNA duplex, after rapid mixing, 20 μl aliquots were taken and manually quenched using 20 μl of 0.5 M HCl at several time points (**Supplementary Figure 2**). An equal volume of phenol/chloroform/isoamylalcohol was then added and the samples were vortexed. The aqueous and organic layers were then allowed to separate by gravity and 80 μl of 2M piperidine was added. Following centrifugation the aqueous layer was transferred to a clean tube and heated for 20 minutes at 90 °C. After heating, both acid- and chase-quenched samples were dried in a vacuum centrifuge and resuspended in 50% formamide containing trace amounts of bromophenol blue and xylene cyanol dyes. The

samples were heated and loaded directly onto a 10% (19:1 bis-acrylamide ratio) denaturing polyacrylamide gel and electrophoresed at 25 watts for 30 min. The gel was dried and exposed to a phosphorimager screen and imaged with a Typhoon 8600 phosphorimager. Gel images were quantified using QuantityOne™ software.

The excision efficiency (E) was calculated using eq S2 (**Supplementary Figure 2**). For a more detailed explanation see Porecha *et al.* and corresponding supplementary methods².

$$E = \frac{k_{\text{ex}}}{k_{\text{ex}} + k_{\text{off}}} \quad [\text{S2}]$$

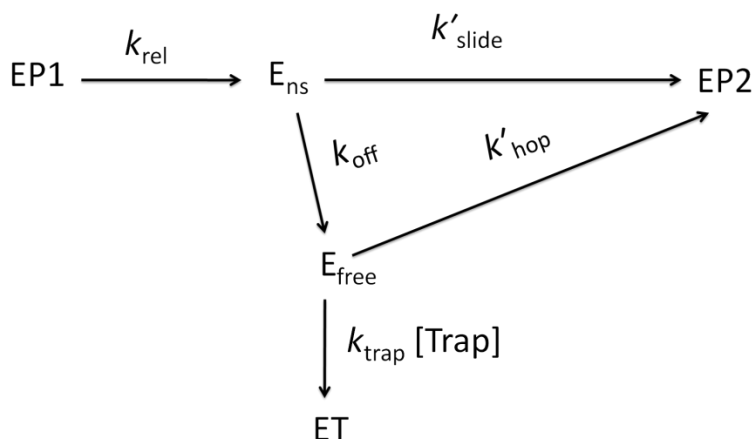
Nonspecific DNA Binding to hUNG

hUNG was titrated into a cuvette containing 50 nM of a 10 bp non-specific DNA duplex (nsDNA) using the same buffer conditions as the intramolecular transfer experiments. The fluorescence anisotropy increase upon hUNG addition was measured using a Spex Fluoromax 3. The dissociation constant (K_D) was obtained by fitting to a single site binding isotherm ($B_{\text{max}} \times [\text{ligand}]_{\text{free}} / (K_D^{\text{ns}} + [\text{hUNG}]_{\text{free}}) + \text{offset}$) in Graphpad Prism 5. In this analysis, the free hUNG concentration was assumed to be equal to the total hUNG concentration due to the greater than 10-fold higher K_D value relative to the concentration of the labeled nsDNA. The binding lifetime to non-target DNA was calculated as $\tau_{\text{bind}} = 1/K_D^{\text{ns}} k_{\text{on}}$. An estimate for the on-rate (k_{on}) of UNG to DNA can be obtained from the diffusion-controlled $k_{\text{cat}}/K_m = 3.4 \times 10^8 \text{ M}^{-1} \text{ s}^{-1}$ (**Supplementary Figure 5**), and previous stopped-flow on-rate measurements using various DNA constructs (2 to $7 \times 10^8 \text{ M}^{-1} \text{ s}^{-1}$)^{1,5}. We employ the value obtained from **Supplementary Figure 5** in the text.

The molecular clock

Theory. The principle of a “molecular clock” has been used previously to measure the lifetimes of unstable reaction intermediates that develop during organic reactions⁶⁻⁸. In the present example, we use a small molecule inhibitor (uracil)^{9,10} to capture free hUNG intermediates that have transiently dissociated from DNA during the process of intramolecular site transfer (**Supplementary Scheme 1**). In the presence of the uracil trap, these

Supplementary Scheme 1



dissociated enzyme molecules can kinetically partition between two pathways: hopping back onto the DNA chain to complete the site transfer and uracil excision process ($k'_{hop} = k_{hop}k_{ex}$), or they will be captured by the trap, which is a second-order process equal to $k_{trap}[trap]$. Accordingly, when $k_{trap}[trap] \gg k'_{hop}$, trapping is 100 % efficient and no dissociated enzyme molecules proceed to the second uracil site by the hopping pathway. It is important to note that even though the enzyme has dissociated from the DNA in order to be trapped, k'_{hop} is *effectively an intramolecular process* because the *same* enzyme molecule hops back onto the *same* DNA chain. Thus, k'_{hop} has the units of s^{-1} .

A useful condition is when the concentration of trap is sufficient to shut down 50% of the hopping events. When this condition is met, $k'_{hop} = k_{trap}[trap]$. A physical interpretation of this particular condition is that uracil diffuses to and traps the free enzyme at the same rate at which the free enzyme diffuses back onto the DNA chain and becomes refractile to trapping. Thus, under this condition the time constant for trapping ($\tau_{trap} = 1/k_{trap}[trap]$) is equal to the time constant for hopping ($\tau_{hop} = 1/k'_{hop}$). As described in the next section, the equivalence of these time constants provides the basis for estimating the characteristic distance traveled by the enzyme before it reencounters the DNA chain during a hopping event of time duration τ_{hop} .

Calculation of the trapping time ($\tau_{\text{trap},0.5}$) and the mean hopping distance ($\langle r_{\text{hop}} \rangle$)

To calculate the trapping time where 50% of the hopping enzyme molecules are trapped by uracil ($\tau_{\text{trap}, 0.5} = 1/k_{\text{trap}}[\text{uracil}]_{0.5}$), we employ the Smoluchowski equation for bimolecular association (eq S3)¹¹. This calculation uses the measured stokes radius of uracil ($r_{\text{u}} = 0.227 \times 10^{-7}$ cm)¹² to calculate a temperature-corrected diffusion constant of uracil ($D_3^{\text{U}} = 1.45 \times 10^{-5}$ cm² s⁻¹ at 37 °C in water), the diffusion constant of hUNG using its stokes radius of 2.3×10^{-7} cm (r_{E}) based on small angle x-ray scattering (SAXS) data ($D_3^{\text{E}} = 1.4 \times 10^{-6}$ cm² s⁻¹)¹³, and Avogadro's number (N_{A}). A value for the fractional binding surface contributed by the active site of the enzyme ($a = 0.3$) was employed, and an electrostatic factor was omitted since uracil is uncharged.

$$k_{\text{trap}} = \frac{4\pi a (D_3^{\text{E}} + D_3^{\text{U}}) (r_{\text{E}} + r_{\text{U}}) N_{\text{A}}}{1000} \quad [\text{S3}]$$

Although uncertainty in 'a' contributes to uncertainty in the calculated value for k_{trap} (and also $\langle r_{\text{hop}} \rangle$, see below), $\langle r_{\text{hop}} \rangle$ is only weakly dependent on 'a' because of its square root dependence on $\tau_{\text{hop}} = \tau_{\text{trap}, 0.5}$ (see **Supplementary Figure 4**). Once k_{trap} is calculated from eq S3 (8×10^9 M⁻¹ s⁻¹), $\tau_{\text{trap}, 0.5} = \{[\text{uracil}]_{0.5} k_{\text{trap}}\}^{-1}$ may be calculated using the concentration of uracil where 50% of the hopping events are trapped (2.1 mM determined from nonlinear least-squares fitting to eq S10). From this approach, a value for $\tau_{\text{trap}, 0.5} = 60$ ns was obtained.

Given that $\tau_{\text{trap}, 0.5} = \tau_{\text{hop}}$ under the condition where 50% of the hopping molecules are trapped, the Einstein equation may be used to estimate the characteristic distance traveled by hUNG in a hopping event of duration τ_{hop} using $D_3^{\text{E}} = 1.4 \times 10^{-6}$ cm² s⁻¹ = 1.4×10^8 nm² s⁻¹ (eq S4).

$$\langle r_{\text{hop}} \rangle = \sqrt{6D_3^{\text{E}} \tau_{\text{hop}}} \quad [\text{S4}]$$

Kinetic description of the intramolecular transfer probability (P_{trans})

Here we derive the kinetic expressions to show how P_{trans} , P_{slide} and P_{hop} are related to the lifetime of hUNG on nonspecific DNA ($1/k_{\text{off}}$), the rate constants for sliding (k_{slide}), hopping (k_{hop}), and the trapping efficiency ($k_{\text{trap}}[\text{trap}]$) (see **Supplementary Scheme 1**). Note that in **Supplementary Scheme 1**, $k'_{\text{hop}} = k_{\text{hop}}k_{\text{ex}}$ and $k'_{\text{slide}} = k_{\text{slide}}k_{\text{ex}}$, where k_{ex} is the uracil excision step. The clock begins after hUNG is released from the abasic site

(EP1) generated from excision of uracil from the first site that is encountered (k_{rel}). Since abasic site dissociation is the rate limiting step during steady-state turnover⁵, none of the subsequent fast steps can be directly measured. However, the partitioning of the enzyme down different kinetic pathways can be ascertained by varying the concentration of the uracil trap, and also from knowledge of the lifetime of hUNG on non-specific DNA. After release from the first site to generate EP1, the enzyme becomes bound to non-specific DNA (E_{ns} , **Supplementary Scheme 1**). From this state hUNG may slide to the next site with a probability (P_{slide}') that is determined by the rate constants for sliding (k'_{slide}) and for falling off the DNA chain (k_{off}) (eq S5). A similar expression describes the probability for falling off the DNA chain (P_{off} , eq S6).

$$P_{slide}' = \frac{k'_{slide}}{k_{off} + k'_{slide}} \quad [S5]$$

$$P_{off} = \frac{k_{off}}{k_{off} + k'_{slide}} \quad [S6]$$

If the site spacing is too large, hUNG will ultimately dissociate to the free enzyme state (E_{free} , **Supplementary Scheme 1**). In the presence of trap, the free enzyme can partition between hopping back on the DNA chain with a probability P_{hop}' (eq S7), or being trapped with a probability P_{trap} (eq S8)

$$P_{hop}' = \frac{k'_{hop}}{k'_{hop} + k_{trap}[trap]} \quad [S7]$$

$$P_{trap} = \frac{k_{trap}[trap]}{k'_{hop} + k_{trap}[trap]} \quad [S8]$$

The total transfer probability (P_{trans}'), as measured in the facilitated transfer assay, is the sum of all pathways leading to EP2, which can be defined in terms of the above probabilities:

$$P_{trans}' = P_{slide}' + P_{off}P_{hop} \quad [S9]$$

$$P_{trans}' = P_{slide}' + P_{off} \left(\frac{k'_{hop}}{k'_{hop} + k_{trap}[trap]} \right) = \frac{k'_{slide}}{k_{off} + k'_{slide}} + \left(\frac{k_{off}}{k_{off} + k'_{slide}} \right) \left(\frac{k'_{hop}}{k'_{hop} + k_{trap}[trap]} \right) \quad [S10]$$

Calculation of the energy barrier for hUNG sliding

Given the experimentally determined one dimensional diffusion coefficient for hUNG sliding to be $6.0 \times 10^3 \text{ bp}^2/\text{s}$ or $6.9 \times 10^{-4} \text{ } \mu\text{m}^2/\text{s}$, the energetic barrier of sliding can be calculated by setting the reference state to that of 'barrierless' sliding as calculated for

rotation coupled diffusion around the DNA helix ($\sim 10^7$ bp²/s, ~ 1 μm^2 /s)^{14,15}. For hUNG sliding we calculate this energy to be approximately 7 k_bT (e.g. $7 k_bT = k_bT \times \ln(D_{1\text{-experimental}}/D_{1\text{-theoretical}})$).

Supplementary Results

Supplementary Figure 1: Binding of hUNG to non-specific DNA in the presence and absence of 10 mM uracil.

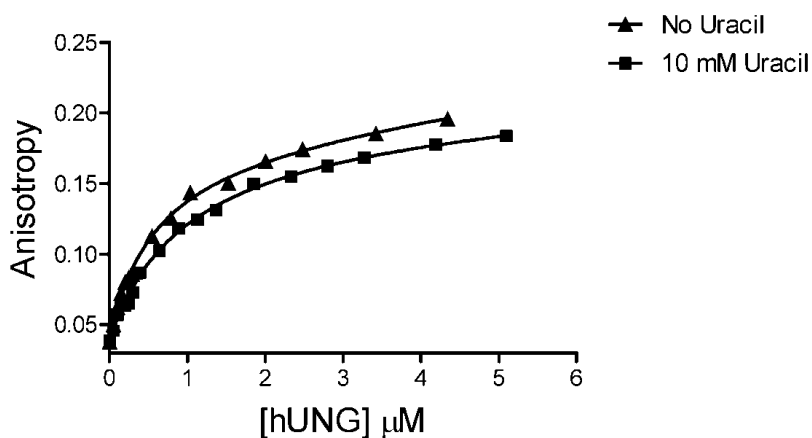
Supplementary Figure 2: Measurement of the efficiency (E) of uracil excision.

Supplementary Figure 3: hUNG transfer versus uracil site spacing in the absence of uracil and comparison with eUNG.

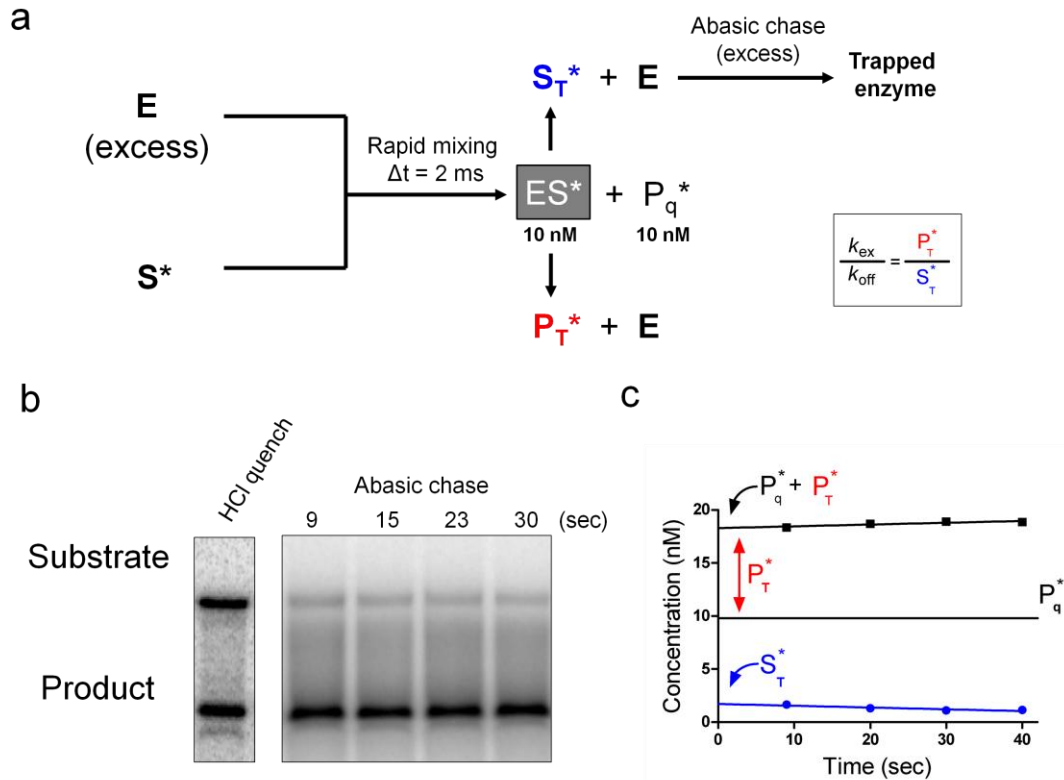
Supplementary Figure 4: Dependence of the targeting radius on the fractional binding surface of hUNG (a) calculated with Smoluchowski equation.

Supplementary Figure 5: Steady-state kinetics of uracil excision by hUNG under conditions of the intramolecular transfer measurements.

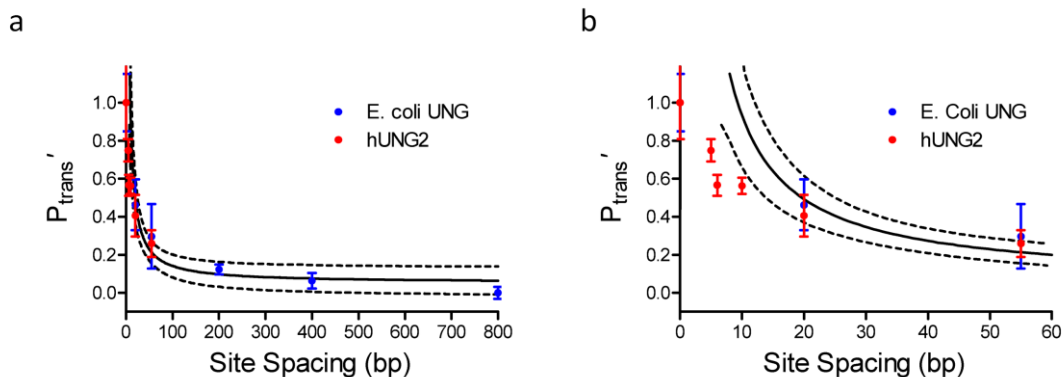
Supplementary Figure 6: Uncut gel images from Figure 2a, b.



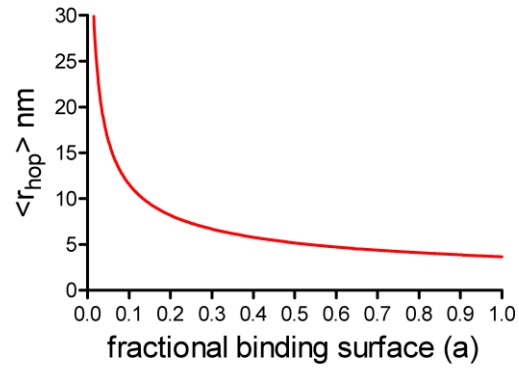
Supplementary Figure 1: hUNG binding to non-specific DNA. hUNG was titrated into a solution containing 50 nM nonspecific DNA duplex (nsDNA, see Methods). Dilution was considered to be negligible and the resulting anisotropy data was fitted to a one site binding model by the non-linear least squares method as described in the Methods. For the binding experiment with and without the addition of uracil K_D values were indistinguishable within error of the measurements ($0.82 \pm 0.26 \mu\text{M}$ and $1.06 \pm 0.13 \mu\text{M}$, respectively). The maximal anisotropy values (B_{max}) were 0.181 ± 0.044 and 0.160 ± 0.012 anisotropy units with and without the addition of uracil. Both data sets were repeated in triplicate and the values listed are the average plus or minus the standard deviation of three independent experiments.



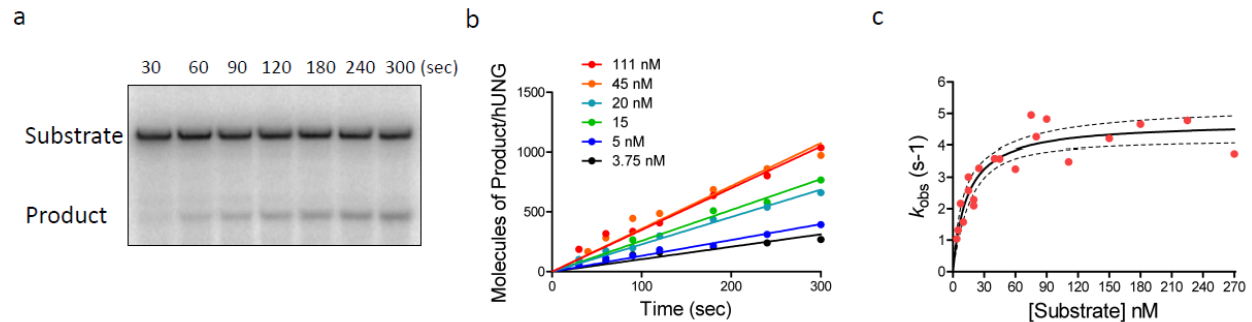
Supplementary Figure 2: Determination of the efficiency of uracil excision (E) (for details see Methods). **(a)** Briefly, hUNG was rapidly mixed with DNA under single turnover conditions (20 nM DNA, 1 μ M hUNG). After an aging time of 2 ms the reaction was quenched directly either by HCl, or alternatively, chased with 60 μ M of the abasic containing chDNA, followed by manual quenching with acid over times ranging between 9 and 40 s post mixing. **(b)** Denaturing gels showing separation of the 5' 32 P-labeled product and substrate after direct acid quench at 2 ms, or during the chase period. **(c)** The amount of product ($P_q^* + P_T^*$) and substrate (S_T^*) remaining after the chase period is depicted by squares and circles respectively. In order to calculate the ratio of k_{ex} to k_{off} and in turn the excision efficiency ($E = k_{ex} / (k_{off} + k_{ex}) = P_T^* / (P_T^* + S_T^*)$), it is necessary to correct for the amount of product already formed within the 2 ms aging time (P_q^*) as determined from the acid quenched samples. Note that since the abasic chase DNA is not 100% efficient, and the possibility exists for the slow unbinding and rebinding of substrate DNA, the value of k_{ex} and k_{off} was calculated using the linearly extrapolated values at zero time of product ($P_q^* + P_T^*$) and substrate (S_T^*). The experiment was repeated five times and E was determined to be $81 \pm 16\%$, where the error represents one standard deviation.



Supplementary Figure 3: Transfer efficiencies for hUNG (red) at increasing site spacings. For comparison are shown the previously measured transfer efficiencies of *E. coli* UNG (blue)². The fitted curve uses a hopping model for intramolecular transfer, where the probability of encountering the second site scales with the size of the site (a) and the inverse of the distance (r) to the site ($P_{hop}' = E \times a/r$)¹⁶. The transfer efficiency at zero spacing (E) is determined by the efficiency of uracil excision by hUNG once it encounters a uracil site (see **Supplementary Figure 2**). The dotted lines display the 95% confidence interval of the fit. For both *E. coli* UNG and hUNG error bars represent one standard deviation and experiments were independently repeated at least three times. Data and fits presented in panels **a** and **b** are the same although the deviation from the $1/r$ hopping model at short spacings is highlighted in panel **b**, suggesting a change in pathway from hopping to sliding at small site spacings.

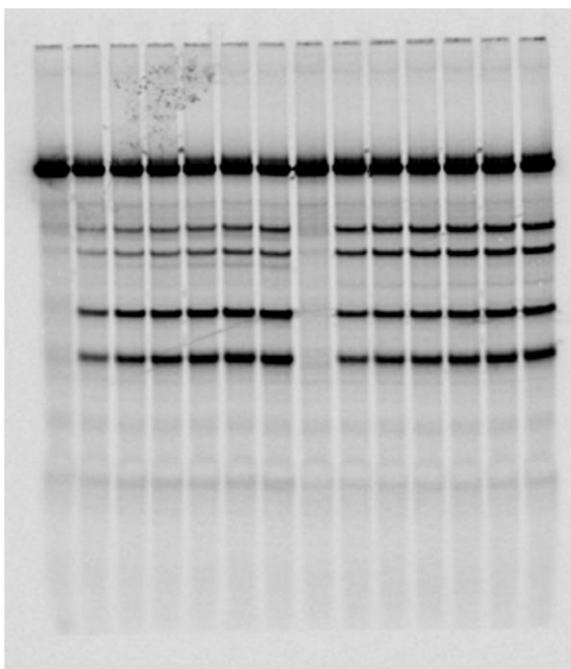


Supplementary Figure 4: Calculated targeting radius ($\langle r_{\text{hop}} \rangle$) based on the Smoluchowski equation (eq S3) and the Einstein equation for a diffusing particle (eq S4) as a function of the fractional binding surface.

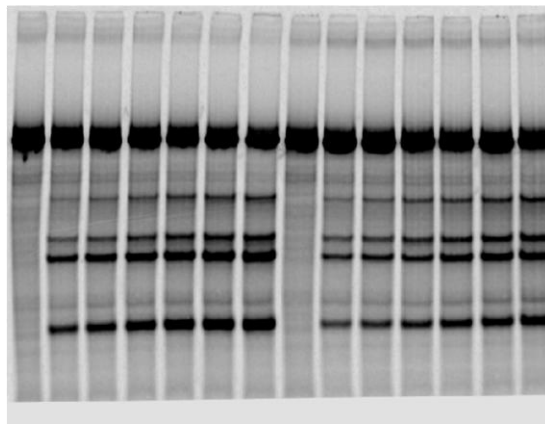


Supplementary Figure 5: Steady-state kinetic parameters for hUNG reaction with a 90 mer duplex DNA substrate containing a single uracil (see Materials and Methods for further details). **(a)** Representative gel analysis showing a reaction time course and resolution of product and substrate species. **(b)** Initial rates of hUNG cleavage at various substrate concentrations. **(c)** Kinetic parameters K_M and k_{cat} were determined to be 13 ± 3 nM and 4.7 ± 0.3 s^{-1} , and $k_{cat}/K_m = 3.4 \times 10^8$ $M^{-1} s^{-1}$. The errors are the standard errors of the non-linear regression fit to the Michaelis-Menten equation.

a



b



Supplementary Figure 6: Uncut gel images from Figure 2a (panel a), and Figure 2b (panel b).

Supplementary References:

1. Krosky, D.J., Song, F. & Stivers, J.T. The Origins of High-Affinity Enzyme Binding to an Extrahelical DNA Base. *Biochemistry* **44**, 5949-5959 (2005).
2. Porecha, R.H. & Stivers, J.T. Uracil DNA glycosylase uses DNA hopping and short-range sliding to trap extrahelical uracils. *Proc. Natl. Acad. Sci. U. S. A* **105**, 10791-10796 (2008).
3. Terry, B.J., Jack, W.E. & Modrich, P. Facilitated diffusion during catalysis by EcoRI endonuclease. Nonspecific interactions in EcoRI catalysis. *J. Biol. Chem.* **260**, 13130-13137 (1985).
4. Zuker, M. Mfold web server for nucleic acid folding and hybridization prediction. *Nucleic Acids Res.* **31**, 3406-3415 (2003).
5. Stivers, J.T., Pankiewicz, K.W. & Watanabe, K.A. Kinetic Mechanism of Damage Site Recognition and Uracil Flipping by Escherichia coli Uracil DNA Glycosylase. *Biochemistry* **38**, 952-963 (1999).
6. Fishbein, J.C. & Jencks, W.P. Elimination reactions of beta-cyano thioethers: evidence for a carbanion intermediate and a change in rate-limiting step. *J. Am. Chem. Soc.* **110**, 5075-5086 (1988).
7. Amyes, T.L. & Jencks, W.P. Lifetimes of oxocarbenium ions in aqueous solution from common ion inhibition of the solvolysis of alpha-azido ethers by added azide ion. *J. Am. Chem. Soc.* **111**, 7888-7900 (1989).
8. Griller, D. & Ingold, K.U. Free-radical clocks. *Acc. Chem. Res.* **13**, 317-323 (1980).
9. Jiang, Y.L., Krosky, D.J., Seiple, L. & Stivers, J.T. Uracil-Directed Ligand Tethering: An Efficient Strategy for Uracil DNA Glycosylase (UNG) Inhibitor Development. *J. Am. Chem. Soc.* **127**, 17412-17420 (2005).
10. Xiao, G. et al. Crystal structure of Escherichia coli uracil DNA glycosylase and its complexes with uracil and glycerol: Structure and glycosylase mechanism revisited. *Proteins* **35**, 13-24 (1999).
11. Smoluchowski, M.V. Mathematical theory of the kinetics of the coagulation of colloidal solutions. *Z Phys Chem* **92**, 129-168 (1917).
12. Nishida, K., Ando, Y. & Kawamura, H. Diffusion coefficients of anticancer drugs and compounds having a similar structure at 30 °C. *Colloid Polym. Sci.* **261**, 70-73 (1983).

13. Timchenko, A.A. et al. Structure of Escherichia coli uracil DNA glycosylase and its complexes with nonhydrolyzable substrate analogues in solution observed by synchrotron small-angle X-ray scattering. *Biofizika* **51**, 5-12 (2006).
14. Schurr, J.M. The one-dimensional diffusion coefficient of proteins absorbed on DNA: Hydrodynamic considerations. *Biophys. Chem.* **9**, 413-414 (1979).
15. Bagchi, B., Blainey, P.C. & Xie, X.S. Diffusion Constant of a Nonspecifically Bound Protein Undergoing Curvilinear Motion along DNA. *J. Phys. Chem. B* **112**, 6282-6284 (2008).
16. Berg, H.C. *Random walks in biology* (Princeton University Press 1993).